Materials Science in Semiconductor Processing 16 (2013) 1888–1893

Contents lists available at ScienceDirect

Materials Science in Semiconductor Processing

journal homepage: www.elsevier.com/locate/mssp

Analysis of Optical properties of nanocrystalline titanium dioxide films

Di Yang*, Ke Wang, Yang Cao, Lei Gao, Xiao Chen, Wenzong Wang

College of Science, Minzu University of China, Beijing 100081, China

A R T I C L E I N F O

Available online 6 August 2013

Keywords:
Complex refractive index
Nano-TiO_2 film
Nanoparticle
Nanotube

A B S T R A C T

The optical properties of materials can be characterized in terms of the complex refractive index. We developed a simple and efficient method for determining the complex refractive index of nanomaterials that uses the relationship between this parameter and the light spectrum measured for a specimen. The optical properties of nanoparticle and nanotube TiO_2 films were investigated. The results show that the morphology of nano-TiO_2 affects the complex refractive index spectrum and therefore influences light dispersion and absorption of the film. We also simulated the optical energy density distribution within equivalent plane films using complex refractive index data.

1. Introduction

Nanocrystalline titanium dioxide (nano-TiO_2) has been widely used in water splitting [1], pollutant degradation [2], and solar cells [3,4]. For these applications, the efficiency of nano-TiO_2 strongly depends on its optical properties [5–7]. Therefore, much research has focused on the optical characteristics of nano-TiO_2 materials such as light scattering, dispersion, and absorption [8,9]. For example, introduction of a light scattering layer into dye-sensitized TiO_2 solar cells effectively improves trapping and absorption of the incoming light and therefore the conversion efficiency of the solar cell.

The optical properties of nanomaterial films can be described in terms of the complex refractive index. The optical absorption and dispersion properties of materials are determined by the relationship between the refractive index and wavelength. Moreover, if the refractive index is known, the optical energy density distribution can be simulated, which is essential for optimal device design. Ellipsometry is a typical method for analysis of the complex refractive index. Moulé et a. used ellipsometry to determine the complex refractive index of porous TiO_2 thin films [10]. However, since the complex refractive index is derived from changes in light polarization in ellipsometry, extraction of the refractive index is complicated. Here we report a simple and efficient method for characterizing the complex refractive index of nanomaterial films. Using this method, we discuss the optical properties of TiO_2 nanoparticle and nanotube films.

2. Experimental

Highly ordered TiO_2 nanotube films were fabricated by anodic oxidation in NH_4F electrolyte, as previously described [11]. TiO_2 nanoparticle films were prepared using a solvothermal approach. First, 0.4 mL of titanium isopropoxide (97%) was added dropwise to 25 mL of ethylene glycol under magnetic stirring. The solution was stirred till it became translucent. It was mixed with 100 mL of acetone and then allowed to stand for 10 h. The powder deposited on the bottom of the vessel was collected and dried at 85 °C in air. Then 0.1 g of this powder was dispersed into a mixture of 12 mL of ethanol and 8 mL of deionized water under strong magnetic stirring. After 10 min of stirring, 0.4 mL of ammonia (28%)

* Corresponding author. Tel.: +86 68933910.
E-mail address: diyang@muc.edu.cn (D. Yang).

1369-8001/$ - see front matter © 2013 Elsevier Ltd. All rights reserved.
http://dx.doi.org/10.1016/j.mssp.2013.06.023

was added to the suspension to obtain the final solution. The mixture was transferred into a 100-mL Teflon-lined autoclave and maintained at 160 °C for 24 h. After cooling to room temperature, the white solid product obtained was washed with deionized water and ethanol several times and then dried in air. Finally, the TiO_2 paste was coated onto quartz glass (JGS1) to a thickness of 1 mm using a scalpel.

The phase structure of the samples was determined by X-ray diffraction (XRD, DX-2200). The morphology was observed using a field-emission scanning electron microscope (SEM, S4800). Transmission and reflection spectra were recorded on a UV-Vis spectrophotometer (Perkin Elmer, Lambda 950). During spectral measurements, incident light was converted to polarized light using a Glan–Thompson polarizing crystal and transmitted light and reflected light were detected by an integrating sphere. The film thickness was measured using a film thickness gauge (NanoCalc-2000-UV/VIS/NIR) and SEM.

3. Theory

A nanomaterial film is a type of non-uniform film and therefore its complex refractive index is in fact the equivalent refractive index. The equivalent refractive index ($N=n+jk$) is analyzed based on the plane film displayed in Fig. 1.

The light field can be resolved into two polarized waves: a TE wave and a TM wave. Since the incident wave is perpendicular to the film in experiments, these two waves have the same Fresnel complex reflection coefficient (r) and transmission coefficient (t) at an interface.

The complex reflectivity can be expressed as $|r|^2 e^{j\phi_r}$ and the complex transmissivity as $|t|^2 e^{j\phi_t}$, where φ_r and φ_t represent the phases created by reflection and transmission at an interface. According to the Fresnel formula [12–14], the amplitude and phase are defined as

$$|r_1|^2 = \frac{(n_0 - n)^2 + k^2}{(n_0 + n)^2 + k^2}, \quad \phi_{1r} = \arctan \frac{-2kn_0}{n^2 + k^2 - n_0^2}, \tag{1}$$

$$|t_1|^2 = \frac{(2n_0)^2}{(n_0 + n)^2 + k^2}, \quad \phi_{1t} = \arctan \frac{k}{n_0 + n} \tag{2}$$

for the top surface, and

$$|r_2|^2 = \frac{(n_2 - n)^2 + k^2}{(n_2 + n)^2 + k^2}, \quad \phi_{2r} = \arctan \frac{-2kn_2}{n^2 + k^2 - n_2^2}, \tag{3}$$

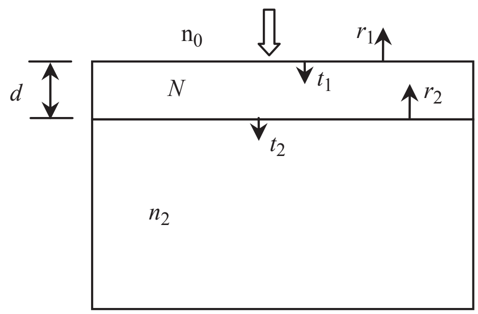

Fig. 1. Plane film of thickness d between a semi-infinite transparent atmosphere (n_0) and a semi-infinite substrate (n_2). r_i and t_i ($i=1$ or 2) represent Fresnel complex reflection and transmission coefficients.

$$|t_2|^2 = \frac{4\left(n^2 + k^2\right)}{(n_2 + n)^2 + k^2}, \quad \phi_{2t} = \arctan \frac{-kn_2}{nn_2 + n^2 + k^2} \tag{4}$$

for the bottom surface. The reflectivity (R) and transmissivity (T) for a plane film can be derived from Eqs. (1)–(4) as

$$R = \frac{|r_1|^2 e^{2\beta k} + |r_2|^2 e^{-2\beta k} + 2|r_1||r_2| \cos(\phi_{1r} - \phi_{2r} + 2n\beta)}{e^{2\beta k} + |r_1|^2 |r_2|^2 e^{-2\beta k} + 2|r_1||r_2| \cos(\phi_{1r} + \phi_{2r} - 2n\beta)} \tag{5}$$

and

$$T = \frac{n_2}{n_0} \cdot \frac{|t_1|^2 |t_2|^2 e^{-2\beta k}}{1 + |r_1|^2 |r_2|^2 e^{-4\beta k} + 2|r_1||r_2| \cos(\phi_{1r} + \phi_{2r} - 2n\beta)}, \tag{6}$$

where $\beta = 2\pi d/\lambda$.

The equivalent complex refractive index can be obtained using these formulas. According to the refractive index obtained, a nano-TiO_2 film can be considered equivalent to a slab and the optical field distribution in the film is easily simulated through the homogeneous Helmholtz equations

$$\nabla^2 \vec{E} + n^2 \left(\frac{\omega}{c}\right)^2 \vec{E} = 0 \tag{7}$$

and

$$\nabla^2 \vec{H} + n^2 \left(\frac{\omega}{c}\right)^2 \vec{H} = 0 \tag{8}$$

We solved Eqs. (7) and (8) using COMSOL software (version 4.2), which is based on the finite element method [15].

4. Results and discussion

The morphology of the TiO_2 films is shown in Fig. 2. The TiO_2 nanoparticle film comprises nanoparticles and nanorods. The thickness was measured as 6.0 μm. The TiO_2 nanotube film consists of nanotube arrays of uniform size and the film thickness is 22.5 μm. The surface roughness of the nanofilms is at the nanometer level and is much less than the thickness, so the films can be considered equivalent to plane films. Fig. 2c shows XRD patterns for the TiO_2 nanoparticle and nanotube films. The peaks at 25.17°, 37.86°, 48.16°, 53.96°, and 62.74° correspond to reflections from the (1 0 1), (0 0 4), (2 0 0), (1 0 5) and (2 0 4) crystal planes, respectively, of anatase TiO_2. It is evident that the major TiO_2 phase is anatase.

Fig. 3a compares measured and fitted transmission and reflection spectra, which clearly overlap. Using the above method, we derived the $n(\lambda)$ spectrum for the quartz substrate from the transmission and reflection spectra and compared them to literature data (Fig. 3b). Few studies have reported the complete $n(\lambda)$ spectrum ranging from 300 to 2000 nm, so data are taken from just two studies [16,17]. The measured and literature data are very close, confirming that the proposed method for determining the refractive index is valid.

Transmission and reflection spectra for samples on a quartz substrate were measured using an integrating sphere detector for the wavelength range 400–1600 nm (Figs. 4a,b). The sum for $T+R$ is slightly greater than 1 at